Journal of Nuclear Materials 392 (2009) 249–254

Contents lists available at ScienceDirect

Journal of Nuclear Materials

journal homepage: www.elsevier.com/locate/jnucmat

Compatibility of FBR materials with sodium

T. Furukawa *, S. Kato, E. Yoshida

Japan Atomic Energy Agency, 4002 Narita, O-arai, Ibaraki 311-1393, Japan

A B S T R A C T

In order to incorporate a procedure for the evaluation of the sodium environmental effects on core and structural materials into the elevated temperature structural design guide lines for fast breeder reactors, R&D on the sodium compatibility of the materials has been in progress in Japan Atomic Energy Agency. This paper reviews corrosion behavior in the sodium of conventional austenitic and ferritic steel. Simultaneously, the corrosion and mechanical properties of the materials for advanced FBRs, 12Cr steel and ODS steels are summarized, including the results of recent research.

1. Introduction

R&D on the sodium compatibility of core and structural materials for the Japanese prototype fast breeder reactor Monju was performed in the 1970s in Japan. The materials are SUS304, SUS316 (including cold-worked steel for the fuel cladding), SUS321 and 2.25Cr–1Mo steel. SUS304, SUS316 and SUS321 are equivalent to AISI type 304SS, 316SS and 321SS, respectively. In the R&D, the effect of temperature, immersion time, dissolved oxygen and sodium velocity on corrosion rate has been estimated. The thermal gradient mass transfer that is a typical corrosion mechanism for the steel in the sodium loop has also been investigated. Based on the research results, a corrosion formula for the Monju design has been determined [1,2]. In order to quantify the effect of sodium on the mechanical properties of the steel, tensile, creep and fatigue tests have been performed in sodium with as-received materials and/or in air with specimens pre-exposed to sodium. A strength reduction factor for Monju design has been given for 2.25Cr–1Mo steel, which is the only material that shows a reduction in strength due to sodium environmental effects [1].

Since the construction of Monju, in-sodium tests of advanced core and structural materials being developed for Japanese demonstration and/or commercial fast breeder reactors (hereinafter referred to as 'advanced FBRs') have been in progress. The materials are FBR grade type 316SS (316FR) [3], high Cr steel (Modified 9Cr–1Mo steel and 12Cr steel [4]) and oxide dispersion strengthened (ODS) ferritic steel [5]. 316FR creep properties are superior to SUS304 and SUS316 at elevated temperatures. High Cr steel has excellent thermal properties compared with conventional austenitic stainless steel, while the mechanical strength is equivalent to the SUS304 and SUS316 steels. This is an advantage due to a reduction in the amount of material required. ODS steel has excellent resistance to swelling as well as superior mechanical strength at elevated temperatures. This steel will be used as the fuel cladding material for long-life fuels in advanced FBRs.

This paper first reviews the corrosion behavior of conventional austenitic and ferritic steel in sodium, and then describes the corrosion and mechanical properties of the materials for advanced FBRs, including recent research results.

2. Corrosion behavior of conventional austenitic/ferritic steel in sodium

It is known that sodium promotes corrosion in two ways. One is corrosion produced by dissolution of alloy elements into sodium, and the other is corrosion produced through a chemical reaction with the impurities in sodium (especially, dissolved oxygen). In a system with a thermal gradient, the former type of corrosion can occur continuously as a function of temperature, temperature gradient and the dissolution and deposition rates of alloy constituents in the sodium loop. The latter type of corrosion can be controlled through impurity control techniques.

Fig. 1 shows the test results for the mass transfer behavior of austenitic steel in flowing sodium. Weight loss (i.e. corrosion) occurs in the high temperature test section due to dissolution of alloy elements into sodium, and weight gain is observed in the low temperature test section by precipitation of the dissolved elements from sodium. According to the metallurgical analysis of sodium piping operated for 100,000 h, the main elements of the mass transfer are chromium, manganese, nickel and silicon [6]. Mass transfer of carbon is also an important factor from the viewpoint of the change of mechanical properties at elevated temperatures. In the case of mono-metallic loops made from austenitic stainless steel, decarburization is not observed at less than 550 °C, which is the maximum temperature of the structural materials used in

* Corresponding author. Tel.: +81 29 267 4141; fax: +81 29 267 0579.
E-mail address: furukawa.tomohiro@jaea.go.jp (T. Furukawa).

0022-3115/$ - see front matter © 2009 Elsevier B.V. All rights reserved.
doi:10.1016/j.jnucmat.2009.03.003

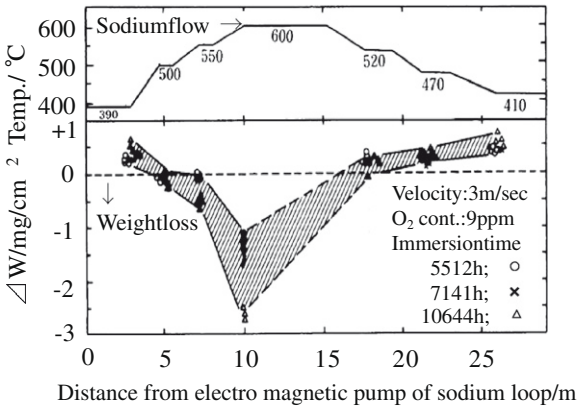

Fig. 1. Weight change in SUS316 after corrosion test in flowing sodium.

advanced FBRs. However, it is observed at the operating temperature of the core materials (max. 700 °C). Snyder reported decarburization on austenitic stainless steel at temperatures above 650 °C with 0.2 ppm of dissolved carbon in sodium [7]. In the case of bimetallic loops such as those found in Monju's secondary cooling system, decarburization occurs in the ferritic steel (2.25Cr–1Mo), the material of the steam generator tubes, and carburization is observed on the austenitic stainless steel (SUS304), the main component of the secondary cooling system. A strength reduction factor for the Monju design is given for 2.25Cr–1Mo steel, the only material that shows strength reduction due to decarburization. Degradation of strength and creep ductility due to carburization is not observed in austenitic stainless steel.

Important factors associated with the environmental sodium effect in steel are (1) immersion time, (2) temperature, (3) dissolved oxygen, (4) sodium velocity and (5) alloy composition. Knowledge about the factors gained from R&D results is summarized as follows:

2.1. Immersion time

The corrosion behavior of austenitic stainless steel in sodium can be divided into two categories: start-up corrosion and steady state corrosion. Start-up corrosion is the result of the selective surface dissolution of elements such as nickel, chromium and manganese into sodium, with metal loss showing a parabolic rate as exposure time increases. Then, the corrosion behavior changes to a lower, approximately constant steady state rate whose mechanism is predominantly general corrosion. The relationship between the corrosion rate and immersion time of austenitic stainless steel is shown in Fig. 2 [8].

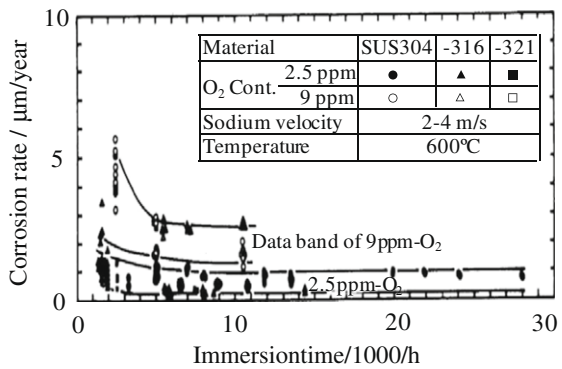

Fig. 2. Relationship between corrosion rate and immersion time.

2.2. Temperature

In a liquid metal system, corrosion is a function of the rate of dissolution or the rate of deposition. The rate of dissolution (CR) is given by the following equation.

$$CR = k(C_s - C_i),$$

where k: solution rate constant, C_s: solubility limit in sodium, C_i: actual concentration in sodium.

k can be diffusion controlled, in which case CR respond to an Arrhenius-like function. Fig. 3 shows the temperature dependence on the corrosion rate of austenitic stainless steel. The steel corrosion rate obtained by the JAEA is within the data band obtained by other researchers [9–14].

2.3. Dissolved oxygen

Because the process is dependent on the chemical reaction with dissolved oxygen in sodium, the effect of dissolved oxygen in sodium on steel corrosion is given by the following equation:

$$CR\ \alpha\ (O_2)^n$$

where CR: corrosion rate, O_2: oxygen concentration in sodium, n: constant.

Fig. 4 shows the relationship between the dissolved oxygen and corrosion rate of austenitic stainless steel. The constant n, estimated by the JAEA is approximately 0.8, and it is equivalent to the values reported by other researchers [8].

2.4. Sodium velocity

The corrosion rate in sodium increases as sodium velocity increases. However, it is reported that the increase ends when the

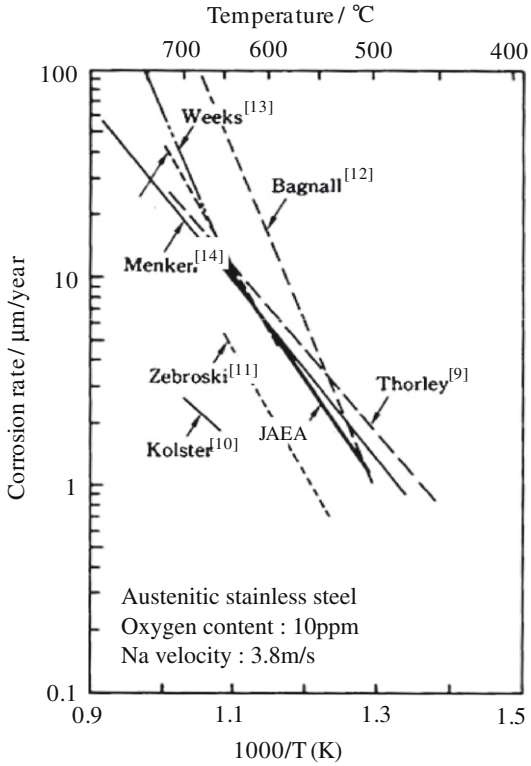

Fig. 3. Relationship between corrosion rate and test temperature.

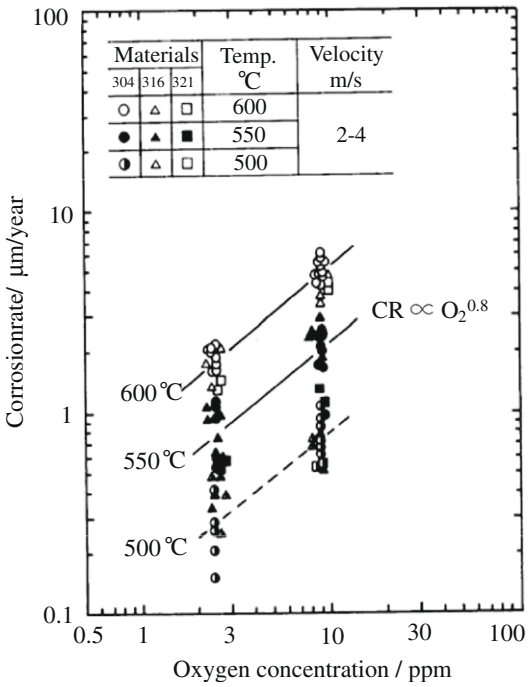

Fig. 4. Relationship between corrosion rate and dissolved oxygen.

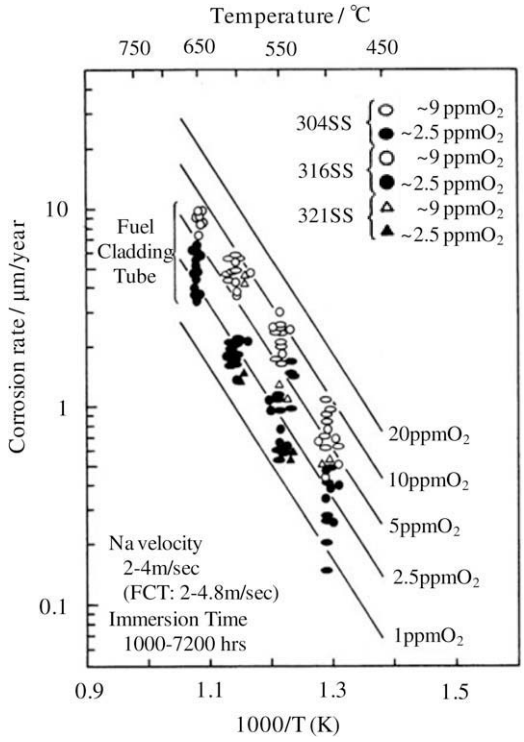

Fig. 6. Corrosion rate of various austenitic stainless steels in sodium.

velocity reaches a certain limit. According to Thorley et al., Roy and Kolster, the limit is described as 3.8 m/s, 6–7 m/s and 3 m/s, respectively [9,10,15]. It is believed that the limit is a function of the oxygen concentration in sodium and/or the structure of the section in sodium.

2.5. Alloy elements

The effect of the alloy elements on corrosion rate is examined because long-term corrosion occurs as a result of thermal gradient mass transfer. The effect of the chromium and nickel contents of steel is particularly significant. As an example, the effect of the nickel content of stainless steel on the corrosion rate is shown in Fig. 5 [15]. However, the dependence of the corrosion rate on alloy elements is seldom observed in austenitic steel such as SUS304, SUS316 and SUS321 due to the fact that the difference of chemical composition is slight (Fig. 6) [15].

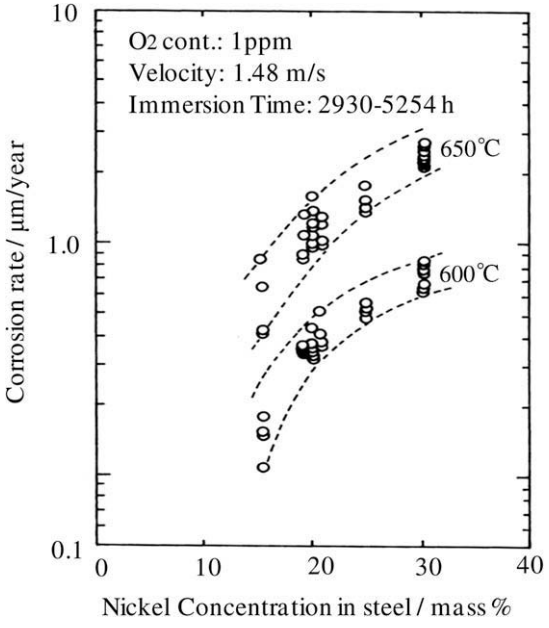

Fig. 5. Effect of Ni content in alloy on corrosion rate in sodium.

2.6. Corrosion formula

Based on the foregoing, the corrosion formula for Monju structure has been determined as follows [1]:

$$\log_{10}R = 0.85 + 1.5\log_{10}Co - 3.9 \times 10^3/(T + 273)$$

where R: corrosion rate, mm/year, Co: oxygen concentration, mass ppm ($5 \leqslant Co \leqslant 25$), T: temperature, °C ($400 \leqslant T \leqslant 650$), materials: SUS304, SUS316, SUS321 and 2.25Cr–1Mo.

In the case of operation at conditions lower than the application range given above, the corrosion rate has to be estimated using the minimum value of the application range.

The corrosion behavior of ferritic steel, 2.25Cr–1Mo steel is different from austenitic steels. However, one corrosion formula has been applied to all high temperature structural materials (austenitic steels and 2.25Cr–1Mo steel) for Monju.

2.7. Mechanical strength in sodium

To quantify the effect of sodium on the mechanical strength of the austenitic / ferritic steel, tensile, creep and fatigue tests in sodium were performed. For austenitic stainless steels, a number of studies have shown that the creep rupture properties can be affected by carburization/decarburization in sodium. However, it was concluded the effect on the mechanical strength was negligible based on the evaluation of the carburization of the stainless steels in the end of reactor operation (approximately 210,000 h, 30 years) [16,17].

On the other hand, 2.25Cr–1Mo steel showed a slight strength reduction due to the decarburization (Fig. 7). Based on the results,

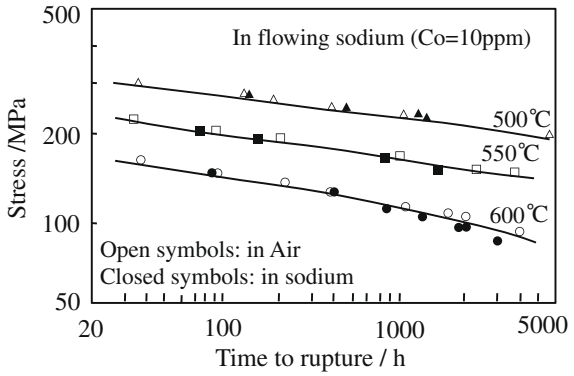

Fig. 7. Creep strength of 2.25Cr–1Mo steel.

a strength reduction factor for Monju design is given for 2.25Cr–1Mo steel only [1].

3. Corrosion and mechanical strength of advanced core and structural materials in sodium

The sodium environmental effect of 316FR and Mod.9Cr–1Mo steel is reported in [18]. The section below describes the sodium environmental effect on other advanced steels, 12Cr steel and ODS steel.

3.1. 12Cr steel

The 12Cr steels, which have mechanical strength superior to Mod.9Cr–1Mo steel and conventional austenitic / ferritic steels at elevated temperatures, has been developed as a structural material for advanced FBRs. The basis of this steel is SUS410J3, developed for thermal power plants. The chemical composition of the tested steel is shown in Table 1.

A corrosion test of this steel in flowing sodium containing 1 ppm dissolved oxygen has been performed at 550 °C for up to 6,000 h. The corrosion behavior was the same as that of conventional austenitic/ferritic steel, and general corrosion was observed on the surface. No local corrosion, such as intergranular penetration, was observed. The corrosion rate at 550 °C was a maximum of 4×10^{-4} mm/year, which is within the band of corrosion data for conventional SUS304 and Mod.9Cr–1Mo steel (Fig. 8).

To quantify the effect of sodium on the mechanical strength of the steel, creep and fatigue tests in sodium were performed. Creep tests were performed at 550 °C in stagnant sodium containing 1 ppm oxygen. The test results are shown in Fig. 9. The creep strength in sodium was equivalent to that in air. In this evaluation, creep tests in carbonized sodium were also performed and no sodium environmental effect was observed. Fatigue and creep fatigue tests were carried out at 550 °C in flowing sodium and/or in stagnant carbonized sodium. The test results are shown in Fig. 10. The fatigue life in sodium was longer than that in air due to the prevention of oxidation. The creep fatigue strength in both flowing sodium and in stagnant carbonized sodium was equivalent to that in air. These results were the same as that of Mod.9Cr–1Mo and conventional austenitic steels which obtained long-term experimental data [19].

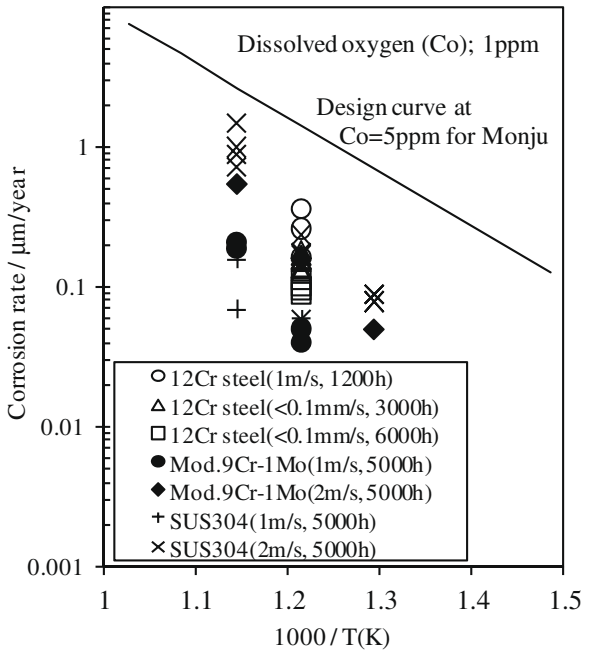

Fig. 8. Corrosion rate of 12Cr and other steels in sodium.

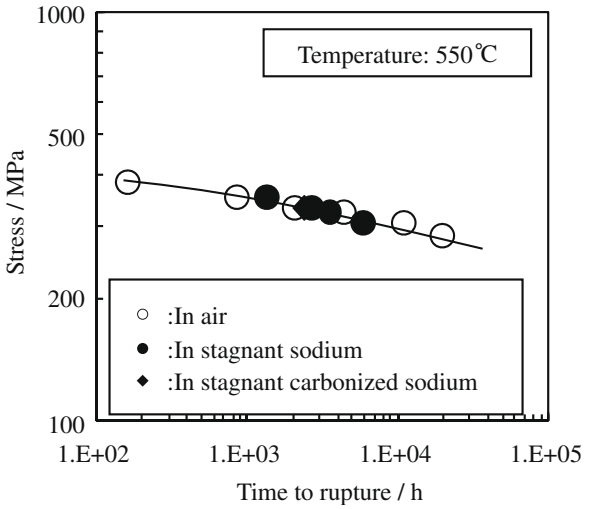

Fig. 9. Creep strength of 12Cr steel.

From the results of the above-reported tests, it was estimated that the effect of sodium on the mechanical strength of 12Cr steel was negligible.

3.2. ODS steel

JAEA has been developing ODS steels as candidate fuel cladding for advanced FBRs since the 1980s. The chemical composition of the candidate steels is fundamentally 9Cr (or 12Cr)–2W–0.2Ti–

Table 1
Chemical composition in mass% of 12Cr steel used for tests in sodium (balance is Fe).

C	Si	Mn	P	S	Cu	Ni	W	Cr	Mo	V	Nb	Sol. Al	N	B
0.11	0.26	0.64	0.016	0.002	1.03	0.39	1.86	10.87	0.31	0.2	0.054	0.001	0.064	34 (ppm)

Normalizing: 1050 °C×1.05 h (AC), tempering: 718 °C × 1.05 h (AC).

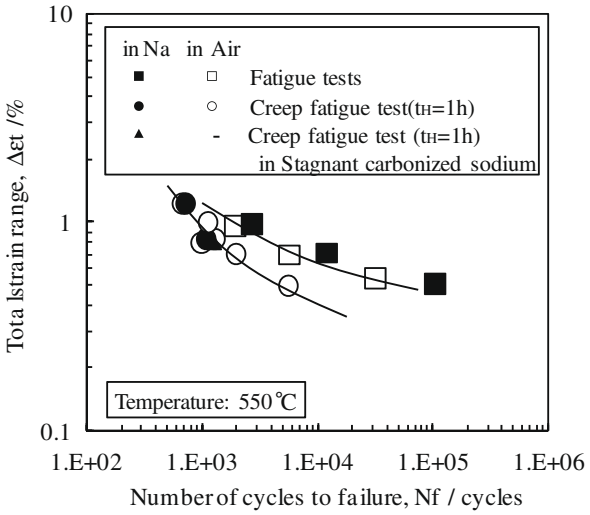

Fig. 10. Fatigue and creep fatigue strength of 12Cr steel.

Table 2
Chemical composition in mass% of various ODS steels tested in sodium (balance is Fe).

	C	Si	Mn	Ni	Cr	W	Ti	Y_2O_3
63DSA	0.02	0.03	0.02	0.12	12.8	2.75	0.74	0.46
F11	0.02	0.05	0.046	0.03	11.95	2.01	0.3	0.24
M11	0.13	0.05	0.044	0.02	9.01	1.95	0.21	0.36
Mm14	0.13	0.0085	<0.01	<0.01	8.835	1.97	0.2	0.35

Estimated from yittrium concentration assuming it is contained in the form of Y_2O_3.

$0.3Y_2O_3$. To date, corrosion tests under two sets of sodium velocity conditions (4.5–5.1 m/s and <0.001 m/s) at temperatures from 600 to 700 °C were performed for the various ODS steels, shown in Table 2. Weight gain caused largely by nickel activity gradient mass transfer from the corrosion test loop structural materials (austenitic stainless steels) via sodium was observed on the materials. This behavior appeared in particular under the high sodium velocity condition and at temperatures above 675 °C [20].

Fig. 11 shows recent results of internal pressure creep tests on cladding tubes in low velocity sodium. The strength in sodium was equivalent to that in inert gas, and no sodium environmental effect was observed. This suggested that the sodium environmental effect could be ignored under low velocity sodium conditions.

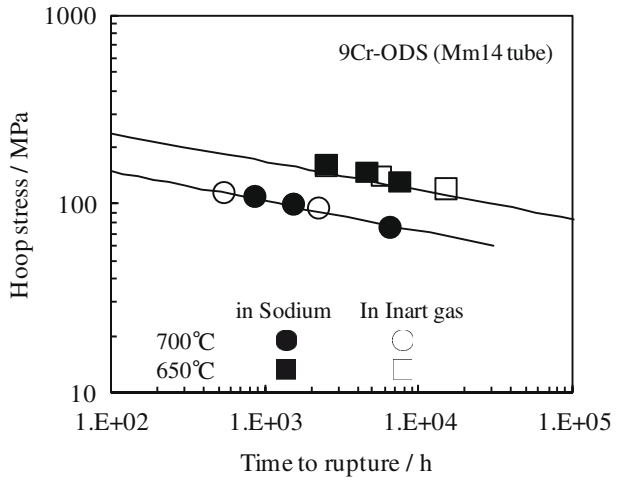

Fig. 11. Creep test results for a 9Cr ODS steel in air and in static sodium.

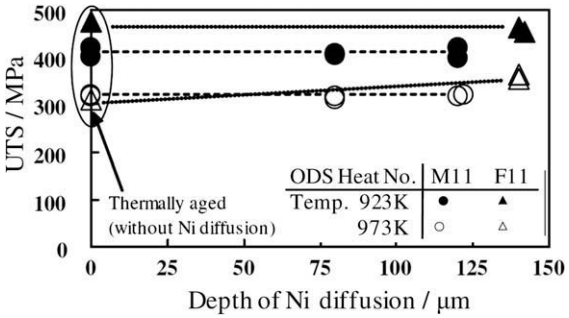

Fig. 12. Influence of Ni diffusion on tensile properties.

However, as the fuel cladding tubes are used under high velocity sodium conditions, it is necessary to consider the effect of microstructural changes associated with nickel mass transfer as observed under high sodium velocity conditions. In order to estimate the effect of nickel diffusion into the ODS steels, tensile tests were performed on artificial nickel-diffused test specimens. The relationship between ultimate tensile strength (UTS) and depth of nickel diffusion are shown in Fig. 12 [20]. The UTS values of nickel-diffused specimens were equivalent to those of specimens that were only thermally aged. It was speculated that the strength of the surface-degraded layer produced by nickel diffusion was probably maintained by the fine Y_2O_3 particles in the steel. It was concluded, in other words, that the effect of nickel diffusion on mechanical strength (tensile strength) was also negligible.

4. Conclusions

The sodium environmental effect on the structural materials used for Monju was reviewed. The important factors associated with the environmental effect on the materials are immersion time, temperature, dissolved oxygen, sodium velocity and alloy composition. Based on the knowledge about the factors gained from R&D results, one corrosion formula has been applied to all high temperature structural materials (austenitic steels and 2.25Cr–1Mo steel) for Monju, although the corrosion behavior of ferritic steel, 2.25Cr–1Mo steel is different from austenitic steels. A strength reduction factor for Monju design was given for 2.25Cr–1Mo steel.

The effect of sodium on corrosion and the mechanical properties of the candidate core and structural materials for the Japanese advanced fast breeder reactor, 12Cr steel and ODS steel, were summarized with inclusion of the most recent test results. The corrosion behavior of 12Cr steel was the same as that of conventional austenitic/ferritic steel, and no effect of sodium on the mechanical strength was observed. On the other hand, weight gain caused largely by nickel activity gradient mass transfer from the corrosion test loop structural materials via sodium was observed on ODS steel under the high sodium velocity condition and at temperatures above 675 °C. However, there was no observed tensile strength reduction of nickel-diffused specimens. It was concluded that the strength of the surface-degraded layer produced by nickel diffusion was probably maintained by the fine Y_2O_3 particles in the steel.

References

[1] K. Iida, Y. Asada, K. Okabayashi, T. Nagata, Nucl. Eng. Des. 98 (1987) 283.
[2] K. Iida, Y. Asada, K. Okabayashi, T. Nagata, Nucl. Eng. Des. 98 (1987) 305.
[3] Y. Wada, E. Yoshida, T. Kobayashi, K. Aoto, in: International Conference on Fast Reactors and Related Fuel Cycles (FR'91), vol. 1, 1991, p. 7.2-1
[4] T. Onizawa, T. Wakai, M. Ando, K. Aoto, Nucl. Eng. Des. 238 (2008) 408.
[5] S. Ukai, T. Kaito, S. Ohtsuka, M. Fujiwara, T. Kobayashi, Mater. Jpn. 45 (2006) 1 (in Japanese).

[6] E. Yoshida, S. Kato, Y. Wada, Post-corrosion and metallurgical analysis of sodium piping materials operated for 100,000 h, Liquid Metal Systems, Plenum press, New York, 1995.
[7] R.B. Snyder, in: Proceedings of International Liquid Metal Technology in Energy Production, Champion, 1976.
[8] A. Maruyama, S. Nomura, M. Kawai, S. Takani, Y. Ohta, H. Atsumo, J. Jpn. Atom. Energy Soc. 26 (1984) 59 (in Japanese).
[9] A.W. Thorley, C. Tyzack, Corrosion and mass transport of nickel alloys in sodium systems, Liquid Alkali Metals, BNES, London, 1973.
[10] R.H. Kolster, in: Proceedings of International Liquid Metal Technology in Energy Production, Champion, PA, USA, 1976, p. 368.
[11] E.L. Zebroski, Liquid Alkali Metals, BNES, London, 1973.
[12] C. Bagnall, D.C. Jocobs, Relationship for corrosion of type 316 stainless steel in liquid sodium, WARD-NA-3045-23, 1975.
[13] J.R. Weeks, in: Proceedings of Symposium on Chemical Aspects of Corrosion and Mass Transfer in Liquid Sodium, 1971, pp. 207–222.
[14] G. Menken, in: Second International Conference on Liquid Metal Technology in Energy Production, XIII-2-3, Richland, 1980.
[15] Sodium Technology Education Committee in JNC, Japan Atomic Energy Agency Public Report, JNC TN9410 2005-011, 2005.
[16] H. Mimura, T. Ito, E. Yoshida, Y. Tsuchida, S. Kano, I. Nihei, in: Proceedings of Fourth International Conference on Liquid Metal Engineering and Technology, vol. 2, Avignon, 1988.
[17] Y. Wada, T. Asayama, R. Komine, Influence of carburizing sodium on cree-fatigue behavior of type 304 steel, in: Proceedings of International Atomic Energy Agency Specialists Meeting on Fast Reactors, KfK 4935 IWGFR/84, 1991, p. 149.
[18] T. Asayama, T. Furukawa, E. Yoshida, ASME PVP 391 (1998) 61.
[19] T. Asayama, Y. Abe, N. Miyaji, T. Furukawa, E. Yoshida, J. Pressure Vessel Technol. 123 (2001) 49–57.
[20] E. Yoshida, S. Kato, J. Nucl. Mater. 329-333 (2004) 1393.